A new technique for the incorporation of seafloor topography in electromagnetic modelling

Kiyoshi Baba* and Nobukazu Seama†

Graduate School of Science and Technology, Chiba University, Yayoi 1-33, Inage, Chiba 263-8522, Japan. E-mail: baba@whoi.edu

SUMMARY

We describe a new technique for incorporating seafloor topography in electromagnetic modelling. It is based on a transformation of the topographic relief into a change in electrical conductivity and magnetic permeability within a flat seafloor. Since the technique allows us to model arbitrary topographic changes without extra grid cells and any restriction by vertical discretization, we can model very precise topographic changes easily without an extra burden in terms of computer memory or calculation time. The reliability and stability of the technique are tested by comparing the magnetotelluric responses from two synthetic seafloor topography models with three different approaches; these incorporate the topographic change in terms of (1) the change in conductance, using the thin-sheet approximation; (2) a series of rectangular block-like steps; and (3) triangular finite elements. The technique is easily applied to any modelling method including 3D modelling, allowing us to model complex structure in the Earth while taking full account of the 3D seafloor topography.

Key words: electrical conductivity, electromagnetic modelling, marine electromagnetic study, topography.

1 INTRODUCTION

Recent geo-scientific interest in electromagnetic (EM) exploration has been focused on more accurate and reliable determinations of the electrical conductivity structure of the Earth, through the progress in modelling methods and improvements in computer performance. In order to obtain more reliable models, *a priori* information, such as topography, should be taken into account. This consideration is especially important for seafloor observations, because the conductivity of seawater is remarkably high, $3.3 \, \mathrm{S\,m^{-1}}$ on average, compared with that of the oceanic crust, which is 10^{-1}–$10^{-3} \, \mathrm{S\,m^{-1}}$ (e.g. Cox *et al.* 1986; Filloux 1987; Evans *et al.* 1994). The flow of electric currents in seawater is distorted by the seafloor topography, and the secondary magnetic field arising from such flows contaminates the observed magnetic fields. In this case, inferring the sub-bottom structure from such electromagnetic field observations is complicated. Since recent technologies (e.g. multi-beam echo-sounding systems) can provide us with detailed seafloor topography, such data should be included in an electrical conductivity model as *a priori* information. Incorporating seafloor topography, however, should not place a severe burden on calculations to model the structure beneath the seafloor, which is the ultimate objective. In this paper, we use 'seafloor topography' to represent relief of the seafloor, and distinguish it from 'bathymetry',

which is frequently used to express the distance between sea surface and seafloor.

To model the effect of seafloor topography accurately but inexpensively has been a long-standing problem for seafloor EM studies. The difficulty mainly arises because the vertical extent of the topographic change is much smaller than the scale of the target substructure and because fine-meshed and 3D numerical modelling needs great computer performance. Until now, two different techniques have been used to incorporate seafloor topography in models. The first technique is the thin-sheet approach, which transforms bathymetry to variable conductance in the sheet (Price 1949). The second technique is to incorporate the geometry of the seafloor directly, using the finite-element method (FEM) or the finite-difference method (FDM).

The thin-sheet approximation is usually applied to the ocean layer, which has variable lateral conductance owing to variations in ocean depth (e.g. Heinson & Lilley 1993; Heinson *et al.* 1993). The conductance of a cell in the sheet is taken as the product of the seawater conductivity and the ocean depth at each position. Heinson *et al.* (1993) applied this method to the seafloor at the Juan de Fuca Ridge area, to estimate the effect of changes in bathymetry, and Nolasco *et al.* (1998) applied the method to Tahiti to remove the effect of the island and the bathymetry from the observations. Although the thin-sheet technique can model 3D bathymetry easily, it has some limitations. First, only 1D structure can be incorporated in the model beneath the sheet because of the difficulties in obtaining an analytical solution to the field equations. This limitation is clearly a major restriction in determining structure beneath the seafloor. Allowing

*Now at: Woods Hole Oceanographic Institution, Woods Hole, MA 02543, USA.

†Now at: Research Center for Inland Seas, Kobe University, Iwaya 2746, Awaji, Tsuna, Hyogo 656-2401, Japan. E-mail: seama@kobe-u.ac.jp

only 1D structures implies that the seafloor is flat and the thin sheet does not include the differences in elevation. Thus, the thin-sheet approximation can model only bathymetry, but may be inadequate for modelling seafloor topography. Secondly, the range of periods for which the thin-sheet approximation holds is limited. This limitation arises from the assumption in the model that the skin depth is large compared with the ocean depth.

There are a number of modelling algorithms using the FEM or the FDM for the 2D situation that can be used to model topography. Wannamaker *et al.* (1986, 1987) modelled topography using the FEM with triangular elements in a 2D magnetotelluric (MT) model, which is suitable for representing the arbitrary geometry of boundary surfaces. Wannamaker *et al.* (1989) applied the algorithm to the EMSLAB data (EMSLAB Group 1988) that were collected across the Juan de Fuca subduction system. Aprea *et al.* (1997) used the FDM for 2D modelling with topography. They were able to treat an arbitrary discrete boundary by replacing the conductivity at each node by an 'effective conductivity', which is an appropriately weighted mean of the actual conductivity surrounding each node. Although these existing methods are effective, it is desirable to take known 3D topography into account as *a priori* information in order to improve the estimation of electrical conductivity structure below the seafloor.

3D modelling with seafloor topography involves several problems. Mackie *et al.* (1994) developed a 3D MT forward modelling algorithm based on the FDM. Using this algorithm, seafloor topography can be represented by steps between rectangular blocks because the algorithm does not model boundaries of arbitrary geometry. In addition, an important point in 3D modelling is that many more grid cells are required to represent the geometry of the seafloor than for modelling a 2D section. As a result, computer memory and calculation time requirements increase dramatically.

This paper describes a new technique for incorporating known seafloor topography in an electromagnetic model. First, we introduce the method, then we tested it. In particular, we add the technique to the 3D modelling algorithm of Mackie *et al.* (1994), and calculate the MT response to two synthetic conductivity structure models. The results are then compared with the model responses calculated by three conventional methods. Finally, we discuss the results and the convenience of our technique.

2 INCORPORATING SEAFLOOR TOPOGRAPHY

We describe our technique for incorporating seafloor topography in this section (Baba *et al.* 1998). The technique is based on a very simple transformation. The seafloor topography corresponds to thickness variations of the ocean and of the underlying crust. We transform these thickness variations into variations in electrical properties and in so doing the seafloor is flattened (we call this the FS technique).

The principles of the FS technique are summarized in Fig. 1. Fig. 1(a) is a sketch of the real Earth. Here, we assume that seawater and crust have homogeneous electrical conductivities σ_s and σ_c, respectively, and a homogeneous magnetic permeability μ_0 for free space (hereafter, the subscripts s and c denote seawater and crust, respectively). This assumption is only for simplicity of explanation and the following arguments are also valid for heterogeneous layers. The actual seafloor topography (Fig. 1a) is discretized into blocks for the modelling (Fig. 1b), as the earth is modelled by blocks. The thickness of the lowermost seawater layer and that of the upper-
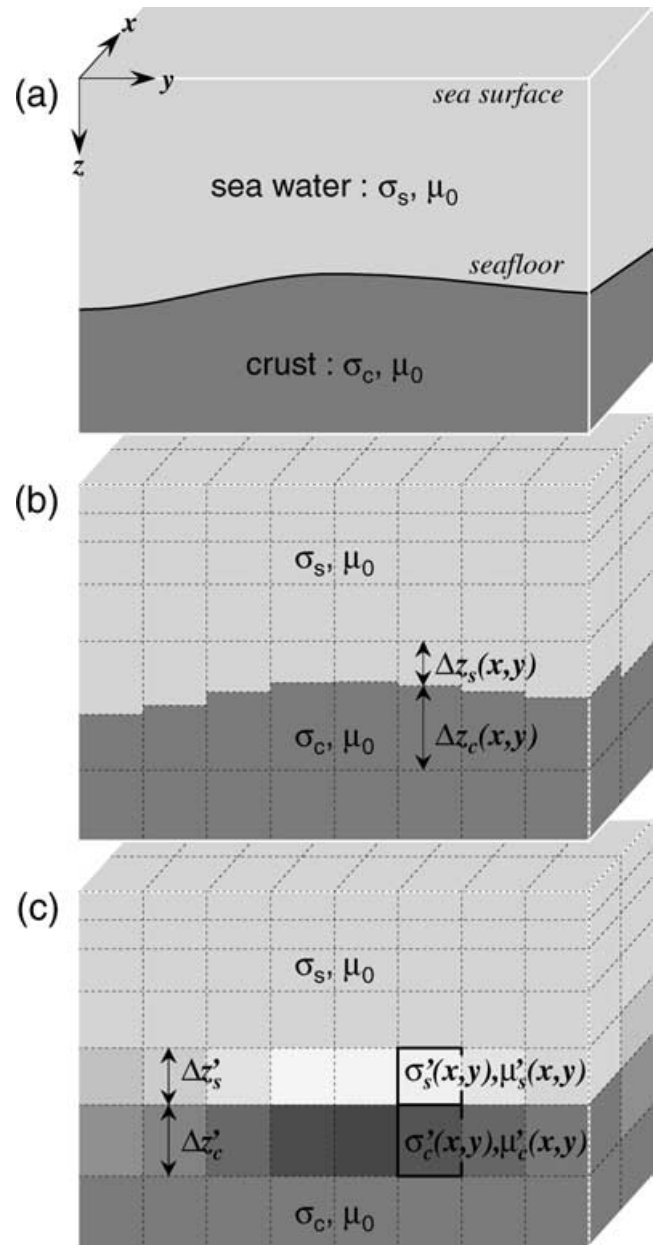
Figure 1. The principles of the FS technique for seafloor topography. (a) Actual topography. Seawater and oceanic crust have constant electrical conductivities σ_s and σ_c, respectively, and a magnetic permeability μ_0. (b) The Earth is divided into rectangular blocks for numerical modelling. The blocks of the layers just above and below the seafloor have variable thickness $\Delta z_s(x, y)$ and $\Delta z_c(x, y)$ with horizontal location (x, y). (c) The conductivity and permeability of the blocks of the two layers are transformed to tensors. Transformed conductivity and permeability vary with horizontal position.

most crustal layer at the horizontal location (x, y), are $\Delta z_s(x, y)$ and $\Delta z_c(x, y)$, respectively. Thus, variations in $\Delta z_s(x, y)$ and $\Delta z_c(x, y)$ represent the relief of the seafloor topography. The representation based on the FS technique is shown in Fig. 1(c). The relief of the seafloor is flattened and $\Delta z_s(x, y)$ and $\Delta z_c(x, y)$ have been transformed everywhere to the constant thickness values $\Delta z'_s$ and $\Delta z'_c$, respectively. From now on, we use a prime to denote variables after the transformation. The σ_s, σ_c and μ_0 values of each block in the layers are transformed to tensors as follows:

$$\boldsymbol{\sigma}'_s(x, y) = \begin{bmatrix} \sigma_s \dfrac{\Delta z_s(x, y)}{\Delta z'_s} & 0 & 0 \\ 0 & \sigma_s \dfrac{\Delta z_s(x, y)}{\Delta z'_s} & 0 \\ 0 & 0 & \sigma_s \dfrac{\Delta z'_s}{\Delta z_s(x, y)} \end{bmatrix} \quad (1a)$$

$$\boldsymbol{\sigma}'_c(x, y) = \begin{bmatrix} \sigma_c \dfrac{\Delta z_c(x, y)}{\Delta z'_c} & 0 & 0 \\ 0 & \sigma_c \dfrac{\Delta z_c(x, y)}{\Delta z'_c} & 0 \\ 0 & 0 & \sigma_c \dfrac{\Delta z'_c}{\Delta z_c(x, y)} \end{bmatrix} \quad (1b)$$

$$\boldsymbol{\mu}'_s(x, y) = \begin{bmatrix} \mu_0 \dfrac{\Delta z_s(x, y)}{\Delta z'_s} & 0 & 0 \\ 0 & \mu_0 \dfrac{\Delta z_s(x, y)}{\Delta z'_s} & 0 \\ 0 & 0 & \mu_0 \dfrac{\Delta z'_s}{\Delta z_s(x, y)} \end{bmatrix} \quad (1c)$$

$$\boldsymbol{\mu}'_c(x, y) = \begin{bmatrix} \mu_0 \dfrac{\Delta z_c(x, y)}{\Delta z'_c} & 0 & 0 \\ 0 & \mu_0 \dfrac{\Delta z_c(x, y)}{\Delta z'_c} & 0 \\ 0 & 0 & \mu_0 \dfrac{\Delta z'_c}{\Delta z_c(x, y)} \end{bmatrix} . \quad (1d)$$

Since $\boldsymbol{\sigma}'_s(x, y)$, $\boldsymbol{\sigma}'_c(x, y)$, $\boldsymbol{\mu}'_s(x, y)$ and $\boldsymbol{\mu}'_c(x, y)$ are functions of $\Delta z_s(x, y)$ or $\Delta z_c(x, y)$, lateral contrasts in the electrical conductivity and magnetic permeability exist in the two layers where the seafloor topography changes.

The transformation of the FS technique changes the scale of the modelling space locally but preserves the Maxwell equations to be solved. The Maxwell equations under the quasi-static approximations are as follows:

$$\oint \mathbf{H} \cdot d\mathbf{l} = \iint \mathbf{J} \cdot d\mathbf{S} = \iint \sigma \mathbf{E} \cdot d\mathbf{S} \quad (2a)$$

$$\oint \mathbf{E} \cdot d\mathbf{l} = \iint i\omega\mu\mathbf{H} \cdot d\mathbf{S}, \quad (2b)$$

where an $e^{-i\omega t}$ time dependence is assumed. An appropriate transformation of conductivity, permeability and field values ensures that eqs (2a) and (2b) remain invariant. Using scaling factors for the transformation to an arbitrary dimension, which are defined as

$$C_x = \frac{\Delta x}{\Delta x'}, \quad C_y = \frac{\Delta y}{\Delta y'}, \quad C_z = \frac{\Delta z}{\Delta z'}, \quad (3)$$

the conductivity, the permeability and the **E**, **H** and **J** fields are transformed to

$$\boldsymbol{\sigma}' = \begin{bmatrix} \sigma \dfrac{C_y C_z}{C_x} & 0 & 0 \\ 0 & \sigma \dfrac{C_z C_x}{C_y} & 0 \\ 0 & 0 & \sigma \dfrac{C_x C_y}{C_z} \end{bmatrix}, \quad (4a)$$

$$\boldsymbol{\mu}' = \begin{bmatrix} \mu \dfrac{C_y C_z}{C_x} & 0 & 0 \\ 0 & \mu \dfrac{C_z C_x}{C_y} & 0 \\ 0 & 0 & \mu \dfrac{C_x C_y}{C_z} \end{bmatrix}, \quad (4b)$$

$$E'_x = C_x E_x, \quad E'_y = C_y E_y, \quad E'_z = C_z E_z, \quad (4c)$$

$$H'_x = C_x H_x, \quad H'_y = C_y H_y, \quad H'_z = C_z H_z, \quad (4d)$$

$$J'_x = C_y C_z J_x, \quad J'_y = C_z C_x J_y, \quad J'_z = C_x C_y J_z. \quad (4e)$$

The conductivity and the permeability become the tensors in this transformation, because conductance and permeance of the media are conserved in the x, y and z directions; the conductance and the permeance in any x, y, z directions are proportional to a section perpendicular to the direction of the gridded blocks and inversely proportional to the distance parallel to the direction of the blocks. Madden & Mackie (1989) applied this transformation to arbitrarily gridded blocks to transform to equally gridded blocks, which can simplify the operator in the difference equation obtained from eqs (2a) and (2b) and simplify the determination of average field values and Earth properties. We apply this transformation to the geometry of the seafloor and we only change the thickness of the blocks so that $C_x = C_y = 1$. Thus, eqs (1a)–(1d) are obtained from eqs (4a) and (4b).

The FS technique has three main advantages. First, it can easily model any seafloor geometry and secondly, it can reduce the number of grid cells required. These benefits result from the FS technique needing only two layers to incorporate seafloor topography by using the above simple transformation. Once we include the FS technique in a modelling method, we can model inexpensively complex (2D or 3D) structures beneath the seafloor, taking full account of the 3D topography, which is difficult for the conventional methods because of their huge computational requirements. Thirdly, the FS technique can be applied to various electromagnetic modelling algorithms.

3 A COMPARISON OF METHODS

We test the FS technique in this section. We include the FS technique in the 3D MT forward modelling algorithm of Mackie *et al.* (1994). The MT responses (apparent resistivity and impedance phase) of two simple synthetic models are calculated using this modelling code. The model responses are compared with those calculated by a number of conventional methods.

3.1 2D example

First example is a 2D synthetic model, which has a 2D seafloor topography (Fig. 2a) over a horizontally layered 1D structure (Fig. 2b). We define a right-hand coordinate system; x is the strike direction, y is the 2D profile direction and z is vertical and increases downwards. The topography is simple so that results can be more easily compared. The depth varies smoothly from 2750 to 3250 m with a sinusoidal dependence between -100 and 100 km in the y-direction, and the maximum gradient of the slope is $0.225°$. The conductivity of the seawater and the oceanic crust are 3.3 and 0.002 S m^{-1}, respectively. The sub-bottom structure consists of the oceanic crust (0.002 S m^{-1}), mantle lithosphere (0.0001 S m^{-1}), asthenosphere (0.1 S m^{-1}) and the underlying mantle is assumed to be a half-space (1.0 S m^{-1}). The magnetic permeability of free space is used throughout.

The methods used for comparison are: (1) the 3D modelling algorithm of Mackie *et al.* (1994) with the FS technique applied; (2) the conventional Mackie *et al.* (1994) algorithm; (3) the 2D modelling algorithm with FEM by Wannamaker *et al.* (1987); (4) the thin-sheet modelling algorithm by McKirdy *et al.* (1985). Hereafter, we refer
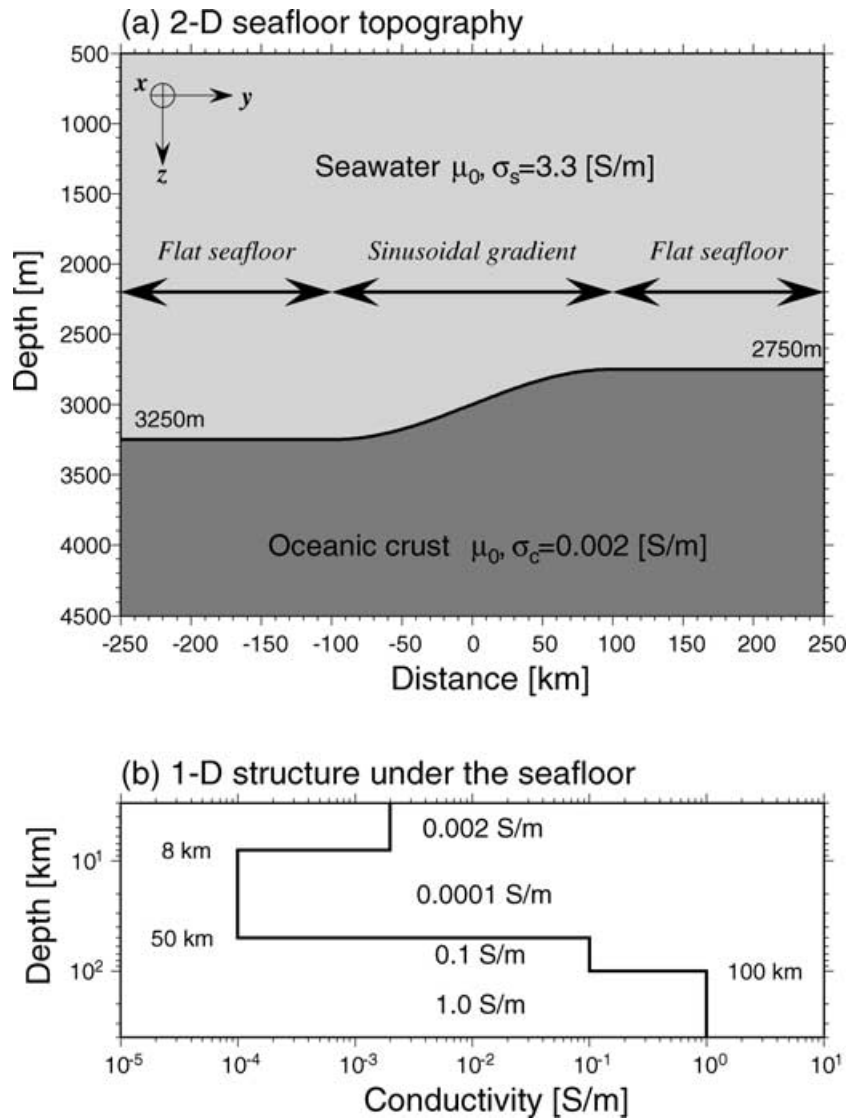
Figure 2. The synthetic electrical conductivity model: 2D seafloor topography model (a) is underlain by 1D layered Earth (b). The depth varies smoothly in the horizontal *y*-direction with a sinusoidal dependence. σ_s and σ_c are 3.3 and 0.002 S m^{-1}, respectively. Free-space magnetic permeability, μ_0, is assumed throughout.

to them as FS3D, FW3D, PW2D and TS, respectively. The seafloor topography is incorporated using the FS technique in FS3D; by a series of steps in FW3D; by triangular elements in PW2D; and by a variable conductance within the thin sheet in TS (Fig. 3). FS3D and FW3D use the same calculation algorithm except for the way in which the seafloor topography is included.

We unify the mesh designs and the electromagnetic field components to be calculated among the four methods as much as possible. Each mesh is designed to have the same calculation points in terms of the *y*-direction, because FW3D and FS3D calculate the electromagnetic fields at grid centres, while TS and PW2D calculate them on grid nodes (Fig. 3). We set the same number of grid cells in the *y*-direction, except in the FW3D case, and in the *z*-direction for the regions shallower than 2000 m and deeper than 4000 m, except in the TS case. In the FW3D case, we set five blocks for each step of the slope region to obtain accurate results—the reason for this will be discussed later. All the MT responses are calculated for horizontal electromagnetic fields at the seafloor for both the transverse electric (TE) and transverse magnetic (TM) modes. Consequently,

we have modified the original PW2D code, which uses the electric field along the slope to calculate the TM mode response.

Results from all four methods agree well on the whole except for the FW3D response on the slope (between −100 and 100 km in the *y*-direction). The apparent resistivity and impedance phase are plotted against position at periods of 1000 s (Fig. 4a) and 10 000 s (Fig. 4b). Apart from this exception, the differences in apparent resistivity between any two methods are almost all within 3 per cent for both modes, and the phase differences are within the equivalent value of 0.86°. The results of the four methods at 10 000 s are more consistent than at 1000 s, especially for the phase.

The FW3D responses on the slope show strange values at both periods. The FW3D apparent resistivity in the leftmost block of each step for the TM mode is severely biased compared with apparent resistivities obtained from the FS3D, PW2D and TS methods. Both the apparent resistivity and the phase for the TE mode also shifted from those by the other methods. The five responses within each step move in opposite directions with respect to the centre of each step. These erroneous effects in FW3D are a result of the
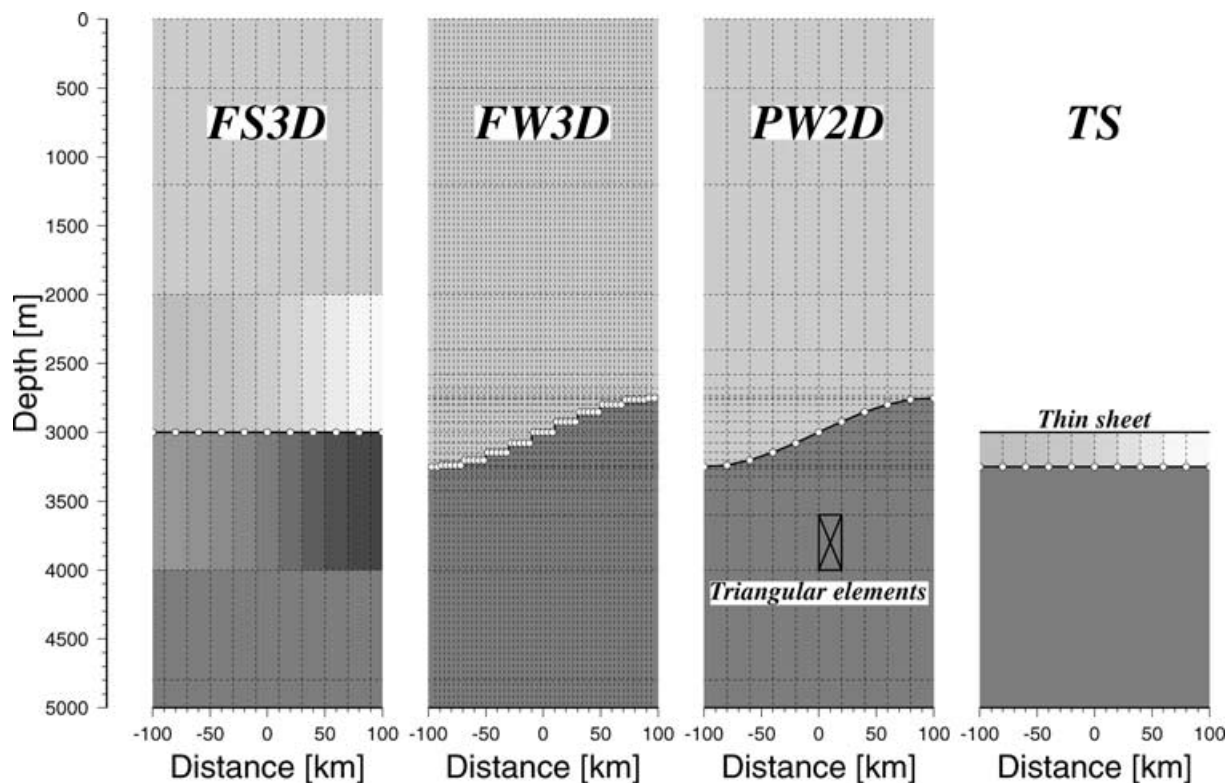
Figure 3. Comparison of modelling of seafloor topography (solid lines) and mesh design (dashed lines) for four numerical methods. The calculation points (circles) are located at the same *y*-positions in the horizontal direction for all methods. The variations in conductivity and permeability are expressed by grey shading on FS3D. For PW2D, each block consists of four triangular elements. For TS, the thin sheet has variable conductance (grey shading), and infinitesimal thickness though shown with a finite thickness. Only the extent between −100 and 100 km in the *y*-direction and less than a depth of 5000 m is shown for all models.

incorporation of the topography as a series of steps. This problem is well known among EM researchers as Aprea *et al.* (1997) have mentioned. When each step contains only one block, the response is averaged and the TE mode response agrees well with those obtained from other methods. The TM apparent resistivity, however, would still be biased because the leftmost response of each step is biased by a large amount. The responses of the centre block of each step agree well with those obtained using the other methods for both the TE and the TM modes. These results suggest that we need to set many grid cells within each step and use the response at the centre block of each step as the response of each step when we incorporate seafloor topography by a series of steps.

3.2 3D example

The second example is a synthetic 3D model that consists of a 3D seafloor topography (Fig. 5a) over the same 1D sub-bottom structure as the 2D example. There are two mountains whose peaks are located at (−40 km, −40 km) and (40 km, 40 km) from the origin (centre of the model), respectively. The mountain at (−40 km, −40 km) is lower in altitude and covers more area than the mountain at (40 km, 40 km). The seafloor changes relatively steeply and abruptly compared with that of the 2D topography model. For the 3D topography model, the maximum gradient of the seafloor is about 1°, which is about four times that of the 2D topography model, and the bathymetry changes from 2000 to 4000 m, compared with 2750 to 3250 m for the 2D topography model. The seafloor topography is discretized in the horizontal direction by cells of dimension 10×10 km^2 (Fig. 5b). The horizontal model space

extends over 1000 km from the origin, although the figure shows only the centre 200×200 km^2. We calculate the MT response by the FS3D and TS methods, and compare the results.

The apparent resistivity and the phase of the four elements at 1000 s calculated using the two methods are shown on maps in Fig. 6. Most maps show similar paterns between the FS3D and the TS responses. The apparent resistivities of the antidiagonal elements (ρ_{xy} and ρ_{yx}) and the corresponding phases (ϕ_{xy} and ϕ_{yx}) are smaller at the tops of the mountains and become larger on the flanks (in the *y*-direction for the *xy* element and in the *x*-direction for the *yx* element) of the higher mountain. For the diagonal elements (ρ_{xx}, ρ_{yy}, ϕ_{xx} and ϕ_{yy}), similar cross-like patterns appear on both mountains.

There are some differences between the responses calculated by the FS3D and TS methods. A relatively obvious difference appears around the origin for both the apparent resistivity and the phase. A higher region of ρ_{xy} (computed by TS) is located with its centre at $x = 50$ and $y = -20$, while the corresponding higher region of ρ_{xy} (computed by FS3D) extends to around the origin. Similar features also appear in ρ_{yx}, ϕ_{xy} and ϕ_{yx}. Furthermore, for the apparent resistivities of the diagonal elements and the phases of the antidiagonal elements changes in the TS response, with respect to location, tend to be smaller than the changes in the FS3D responses.

4 DISCUSSION

The above MT responses for the 2D seafloor topography model also underline the importance of modelling seafloor topography. We use small and gentle topography for the model (Fig. 2); the amplitude
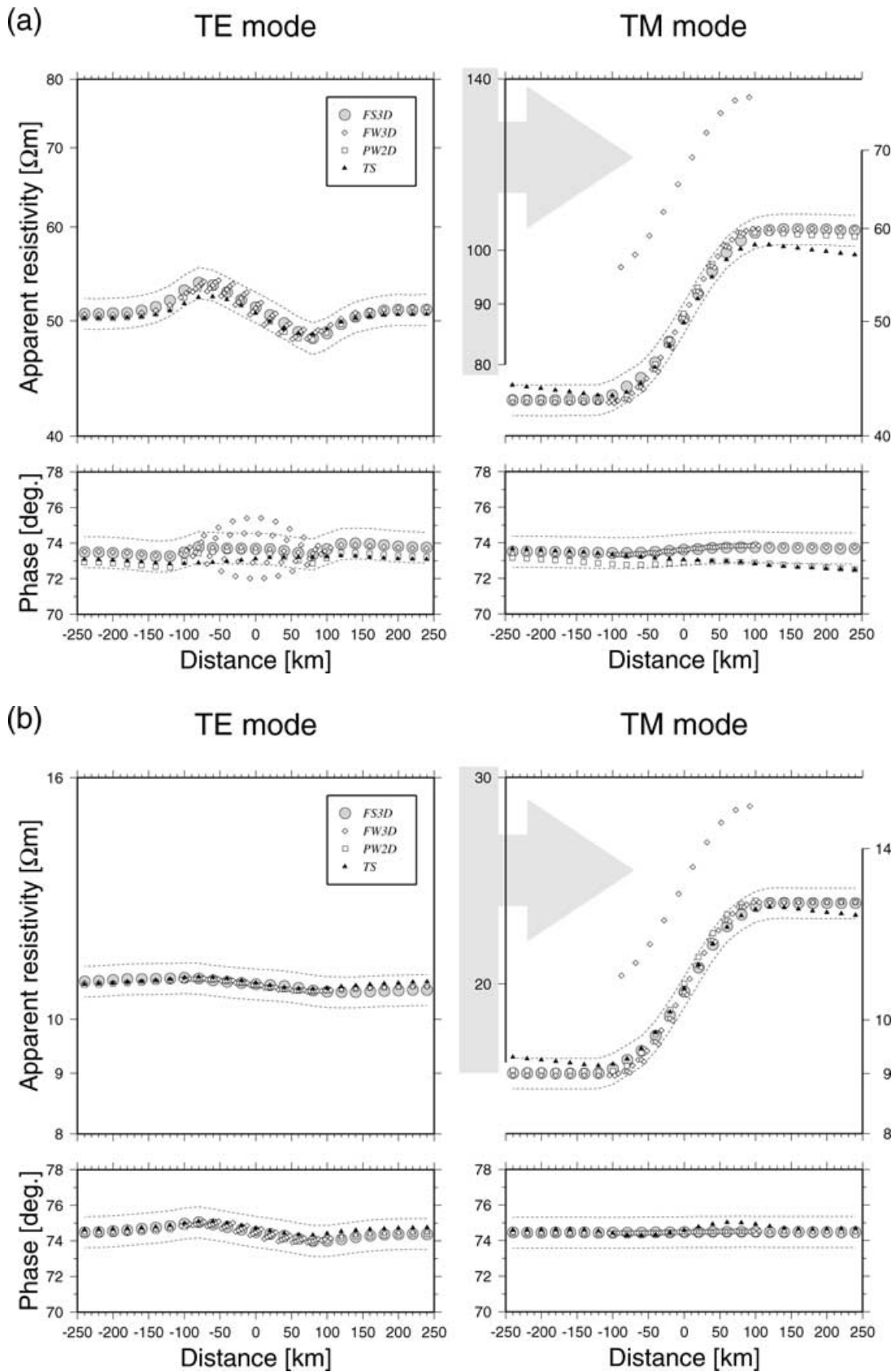
Figure 4. Computed MT responses by the four methods at (a) 1000 s and (b) 10 000 s for the model shown in Fig. 2. Dashed lines are ±3 per cent of the FS3D response in apparent resistivity and equivalent values of ±0.86° in phase. The same logarithmic scale is used for plotting all the apparent resistivity curves. Note that the FW3D apparent resistivity for the TM mode between −100 and 100 km (just over the slope) is plotted against the vertical divisions on the left-hand side and the other apparent resistivities against the vertical axis on the right.
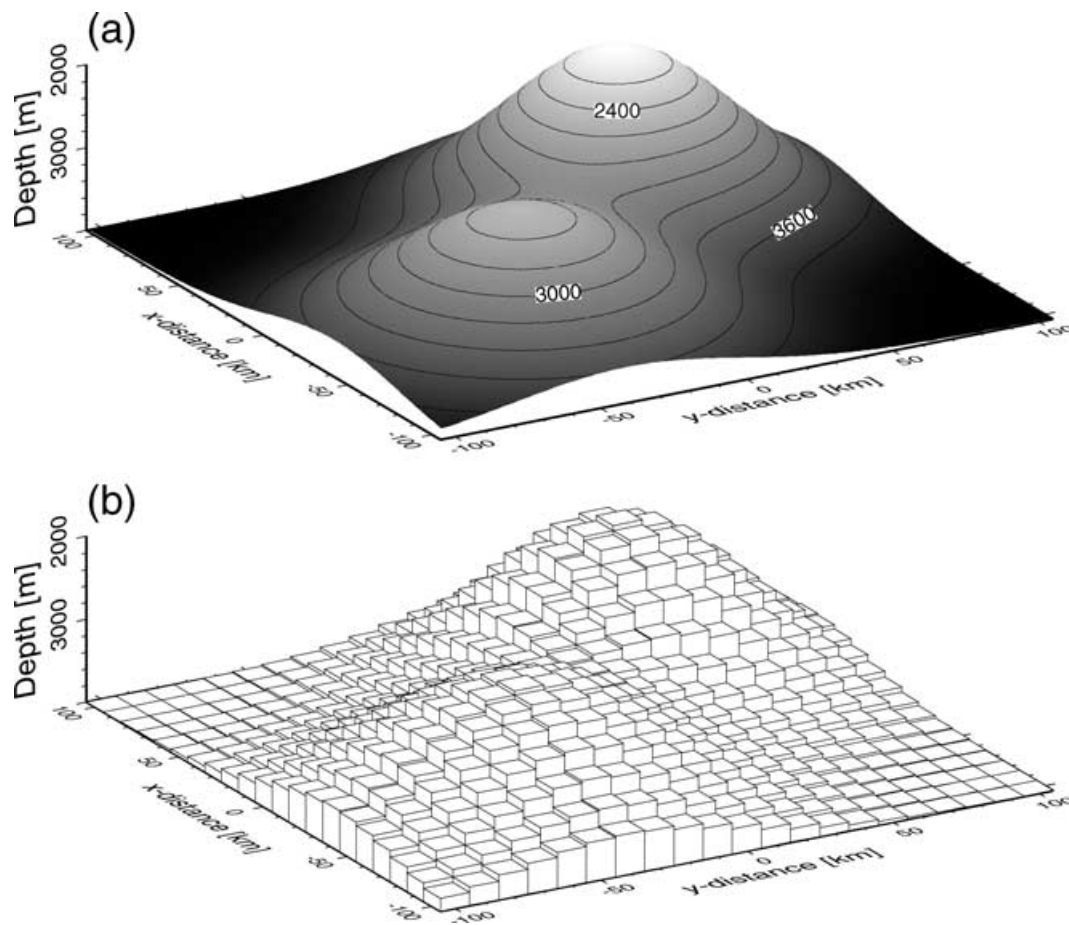
Figure 5. (a) 3D seafloor topography model and (b) its discretized feature for the numerical calculations.

of the topographic variation, 500 m, is very small compared with the skin depth for the seawater (about 9 km at 1000 s). Even such a slight seafloor topography manifestly affects the MT response, especially for the TM mode, which suffers from galvanic or boundary charge contributions. The variation in the apparent resistivity of the TM mode along the *y* axis at 1000 s is about ±17 per cent of the mean value, while that for the TE mode is ±4.6 per cent (Fig. 4a). The TM mode variation at 10 000 s is still about ±17 per cent, although the TE mode variation is reduced to a very small value (Fig. 4b). The results indicate that even small variations of seafloor topography affect the data at all periods for the TM mode, while they only affect the data at shorter periods for the TE mode. Without incorporating the seafloor topography in a model, we may erroneously attribute effects of this topography on the observed data to the sub-bottom structure. Thus, seafloor topography, which is well known, must be incorporated in the model to prevent such an incorrect estimation and to estimate the sub-bottom structure more reliably.

We have shown that the FS3D method is as reliable as the conventional modelling methods through comparisons with the responses calculated by those methods. The responses of the 2D topography model, calculated by the different methods, agree well and the small differences in response between the methods are probably a result of the differences in the calculation algorithms. The FS3D responses differ by 0 to 3 per cent in apparent resistivity and phase from the PW2D or the TS responses. Similar differences exist between any other combinations of results. However, the FS3D response is much closer to the FW3D response when we consider the FW3D response of the centre block for each step with the FW3D response over the

slope. The difference in the TE mode apparent resistivity is within 1 per cent and the phase difference is nearly 0° at all positions. The differences for the TM mode apparent resistivity and phase are smaller compared with the difference between the PW2D or the TS methods. Since FS3D uses exactly the same calculation algorithm as FW3D, except for the way in which the seafloor topography is included, the difference among the responses of the four methods probably indicates a difference in these calculation algorithms. We understand that comparison with analytical solutions is an ideal way to check the accuracy of the FS3D calculation, but it is very difficult to obtain analytical solutions even for the simple topography models we have used here. The comparison with various conventional methods is a reasonable way to check the accuracy, even if each method may have uncertainties in its calculations. The comparison leads to the conclusion that the FS3D calculation is accurate to within the uncertainty arising from the differences in the numerical algorithms and that the FS technique is effective.

The FS technique involves no restriction on modelling either the 2D or the 3D seafloor topography from a theoretical point of view, but we make a preliminary comparison between the FS3D and the TS calculations to assess the reliability of the 3D calculation, even if we cannot determine the accuracy of the TS calculation. The responses for the 3D topography model using the FS3D and TS methods show mostly similar patterns, although relatively larger differences appear than for the 2D topography model. The differences occur mainly as a result of the unstable calculation of the TS method. We check the stability of the numerical calculation of the FS3D and TS methods using the symmetry of the 3D topography
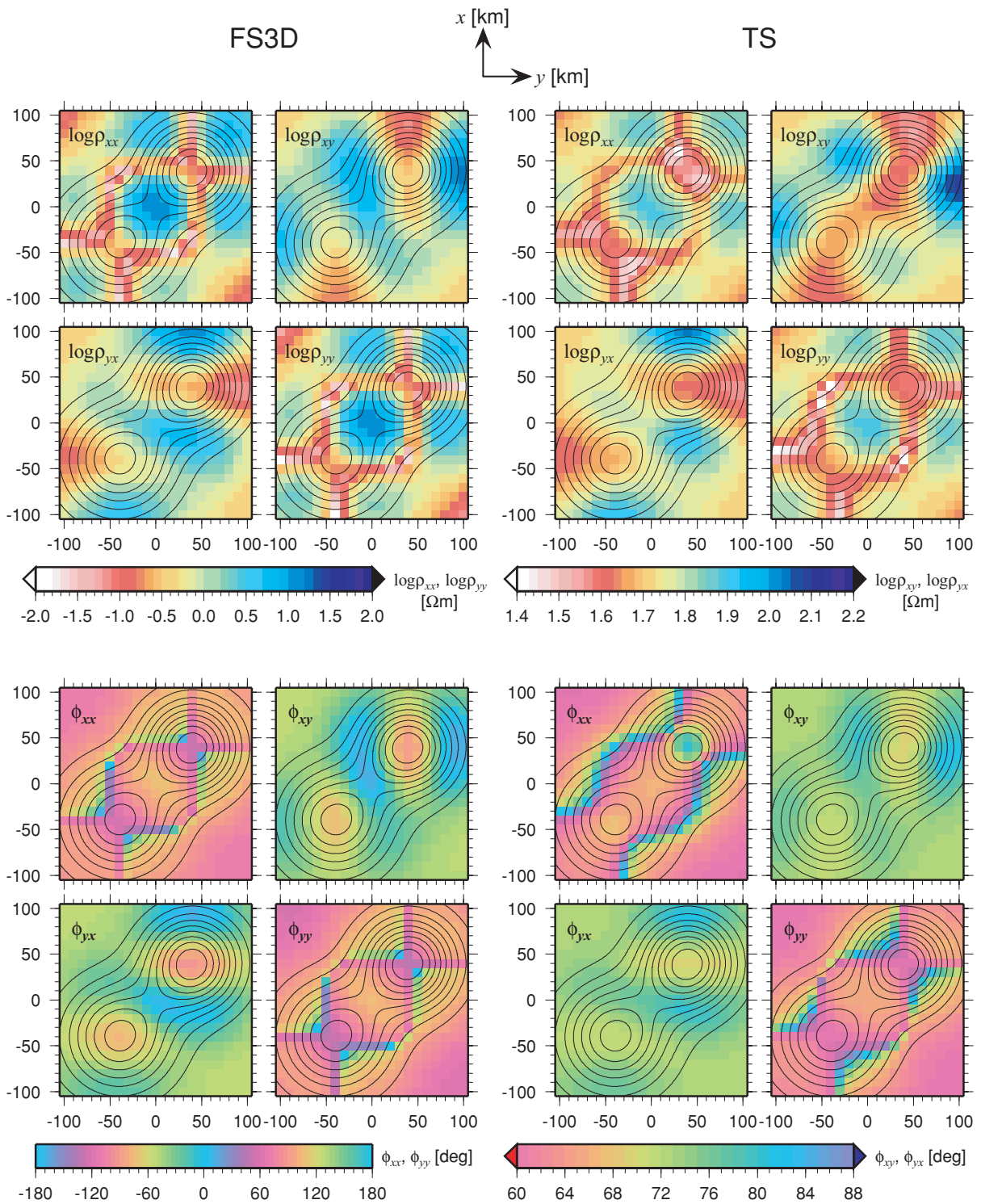
Figure 6. Model responses at 1000 s calculated by FS3D (eight panels on the left-hand side) and TS (eight panels on the right-hand side) superimposed on the bathymetry map. Colours indicate the values of the log apparent resistivity and phase, but different palettes are used for diagonal and antidiagonal elements. The contour lines of the bathymetry are drawn with 200 m intervals. The horizontal and vertical scales of the panels show the distance in kilometres.

model. Since the 3D topography model is symmetric with respect to the line of $y = x$, the model responses for the xy and the yx elements are symmetric about the line. For example, ρ_{xy} along the line $y = a$ should be same as ρ_{yx} along the line $x = a$, where a is an arbitrary distance from the origin. ϕ_{xy} along the line $y = a$ should also be the

same as ϕ_{yx} along the line $x = a$ with a shift of $180°$ which is physically the same. The xx and the yy elements have the same relation. The model responses along the lines $x = 0$ and $y = 0$ are plotted in Fig. 7. Large and small symbols represent the symmetric responses and should agree when the calculation is exact and stable. The
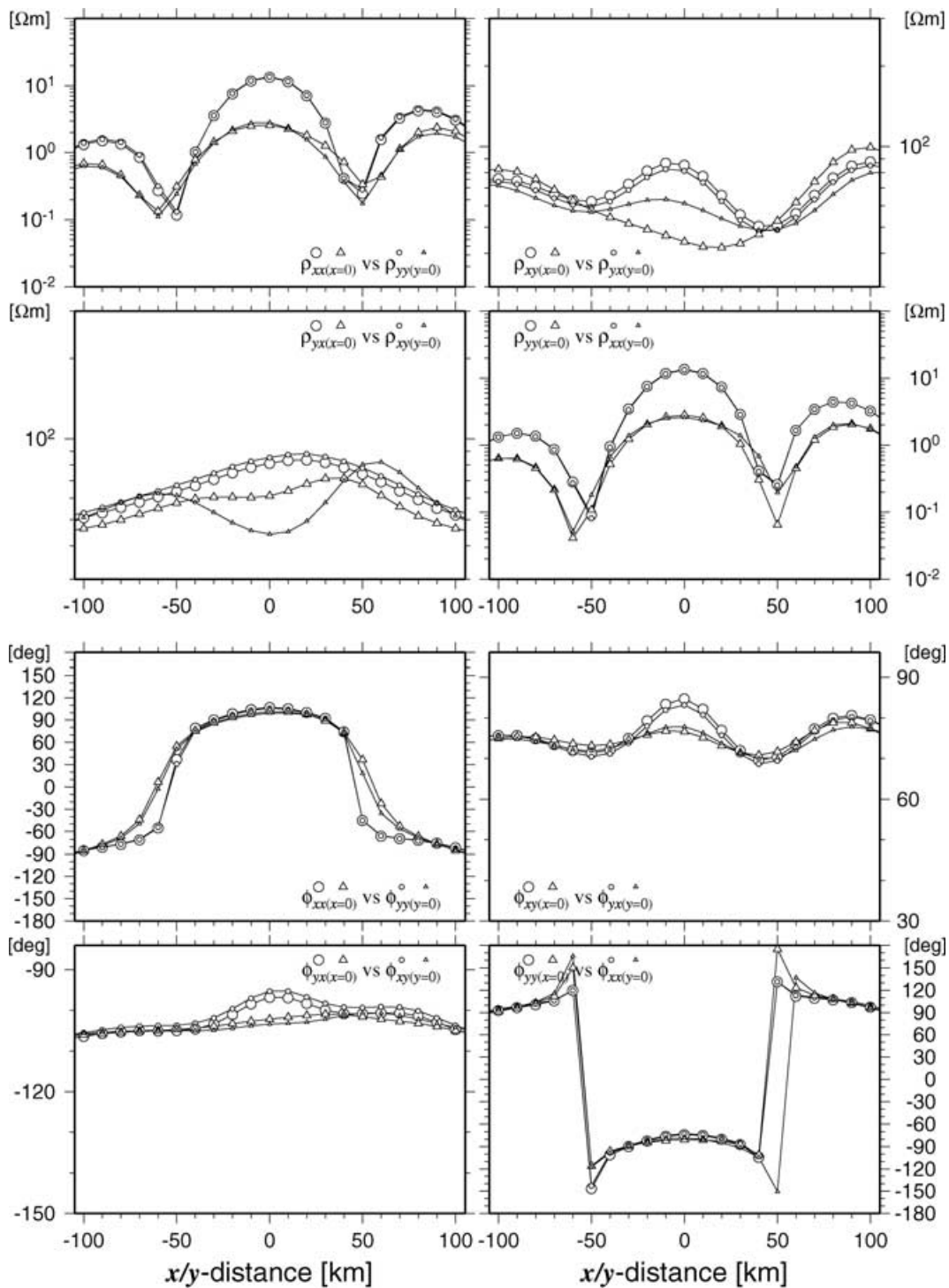
Figure 7. Comparison of the FS3D (circles) and the TS (triangles) responses including symmetric responses owing to the symmetry of the seafloor topography model (Fig. 5). Large symbols are the response along the line $x = 0$ and small symbols are the symmetric response along the line $y = 0$, as annotated in each panel. For example, ρ_{xy} along the line $x = 0$ and ρ_{yx} along the line $y = 0$ calculated by both FS3D and TS are plotted in the upper right-hand panel. The symmetric phases are shifted by $180°$ to appear in the same quadrant. See the text for further details.

results indicate that the symmetric responses computed by FS3D agree much better than those computed by TS. The symmetric values of ρ_{xy} and ρ_{yx} differ greatly around the origin for the TS case, indicating that the FS3D calculation is more stable than the TS calculation. There are relatively large differences in the response in spite of both methods being stable. For example, although the symmetric values of ϕ_{xy} and ϕ_{yx} agree well for each method, the FS3D

phases are about $8°$ larger than the TS phases around the origin. Similarly, ρ_{xx} and ρ_{yy} values differ between the FS3D and the TS methods. It is difficult to evaluate the accuracy from a comparison with a single conventional method. We cannot judge which result is more accurate or whether these differences are in a permissible range for the algorithms. However, we cast doubt on the TS results, especially for ϕ_{xy} and ϕ_{yx}, because the corresponding ρ_{xy} and ρ_{yx}

values computed by TS are unstable. Thus, we suggest that the FS3D method is more reliable than the TS method as far as the stability of the calculation is concerned, and that the FS technique is effective even for the 3D case.

We confirm two advantages of the FS technique in practical use in Fig. 3. These are much easier mesh design and a reduced number of grid cells, because the FS technique needs only two layers to model the seafloor topography owing to the transformation of eqs (1a)–(1d). The FS technique allows us to design meshes easily for any topography. We first set up the mesh layering so that all of the topographic change is accommodated within two layers, and then we set the horizontal intervals freely although we must avoid large differences in size between adjacent blocks. The tensor conductivity and permeability are automatically calculated from the depth. It is worth noting that the depth can be set to arbitrary values without any restrictions being imposed by the vertical discretization. On the other hand, conventional methods (FW3D and PW2D) require further troublesome work for mesh generation. We need to adjust the mesh intervals both in the horizontal and in the vertical directions simultaneously so that the seafloor passes as nearly through the grid nodes as possible. Such work is much more complicated with complex topography.

The FS3D method reduces the number of grid cells compared with the FW3D and PW2D methods. In the 2D topography model, FW3D and PW2D use 10 layers to model the slope and an extra five layers are required both above and below the bounding layers, because the size of the blocks should not change abruptly. Only two layers between depths of 2000 and 4000 m are required for FS3D, but 20 layers are required for FW3D and PW2D. Since the total numbers of layers are 17 for FS3D and 26 for FW3D and PW2D, FS3D saves 35 per cent in grid cells in the *z*-direction. Furthermore, the FW3D method needs a much finer mesh in the horizontal over the slope to obtain accurate results, as already mentioned. To model the topography more precisely, we must make the grid intervals small both in the horizontal and in the vertical directions for FW3D and PW2D, but only in the horizontal for FS3D. In this case, the reduction in the number of grid cells grows larger, leading to savings of both computer memory and calculation time.

The successful FS3D calculation, where the FS technique is included in the 3D MT modelling based on FDM, indicates the effectiveness of the FS technique. This technique is not restricted to a single numerical method, because it incorporates the geometry of the seafloor in a model without changing the Maxwell equations to be solved and is not the technique used to solve these equations. Thus, it should be easy to include the FS technique in other algorithms and it can be applied to all electromagnetic problems including the MT problem. This is the other advantage of the FS technique.

Two practical limitations of the FS technique exist. In the situations where bathymetry changes greatly or the model contains a coastline, the FS technique obviously cannot be applied directly. When bathymetry changes greatly, the two layers applied to the FS technique becomes thicker. Generally, coarse discretization reduces the accuracy of the numerical calculation. The scale of the discretization is based on the skin depth for the modelling of the geomagnetic induction problem. The thickness of the layers should be sufficiently less than the skin depth of the ocean, which is ∼8.8 km for 1000 s and ∼2.8 km for 100 s, and it may limit the thickness of the two layers applied to the FS technique. Furthermore, when the model contains a coastline, i.e. a water depth of 0 m, we cannot set the two layers containing seawater and crust to extend completely across the horizontal extent of the model. These limitations can be overcome when we need the model response only in regions of in-

terest. We apply the FS technique only to the region of interest and use other methods, a series of steps for example, outside the region. Even when we use a series of steps outside the region, we can obtain an accurate model response in the region of interest, because the incorrect model response owing to a series of steps only appears at the location of the steps and the response away from the steps is almost the same as the response computed using the other methods (Fig. 4). Other limitations of the FS technique may occur because the practical usage of the FS technique is related to many parameters, for example, the mesh scale both in the vertical and horizontal directions, the thickness of the two layers applied to the technique, the range of topographic change, the topographic gradient and so on. However, even if these practical limitations do occur, they should be overcome through further experience, because the FS technique is based on a simple clear idea and has no weakness from a theoretical point of view.

5 CONCLUSIONS

The seafloor topography greatly contaminates the electromagnetic field observed on the seafloor. We emphasize that taking account of the seafloor topography in electromagnetic modelling is very important to estimate reliably the conductivity structure model beneath the seafloor and that establishing a method to include the seafloor topography accurately but inexpensively in numerical models has been a perennial problem for marine EM researchers.

The FS technique is proposed as a new way to incorporate seafloor topography in electromagnetic modelling. The FS technique is based on a very simple idea and offers the advantages that it can model any geometry of the seafloor easily, it can reduce the number of grid cells, and it can be included in a range of algorithms used for modelling calculations. The FS technique provides a solution to the problem of modelling actual seafloor topography, without increasing the computational load.

We have included the FS technique in the 3D MT forward modelling algorithm by Mackie *et al.* (1994). Comparisons with conventional modelling methods indicate that this FS3D method calculates reliable responses to the seafloor topography. FS3D can model a 3D conductivity structure in the Earth, taking full account of the 3D seafloor topography and is useful for estimating more reliable structure from observations, even if the observations are contaminated by seafloor topography.

REFERENCES

Aprea, C., Booker, J.R. & Smith, J.T., 1997. The forward problem of electromagnetic induction: accurate finite-difference approximations for two-dimensional discrete boundaries with arbitrary geometry, *Geophys. J. Int.,* **129,** 29–40.

Baba, K., Seama, N. & Masaki, Y., 1998. 3D electromagnetic modeling including seafloor topography, *EOS, Trans. Am. geophys. Un.,* **79,** 228.

Cox, C.S., Constable, C.S., Chave, A.D. & Webb, S.C., 1986. Controlled-source electromagnetic sounding of the oceanic lithosphere, *Nature,* **320,** 52–54.

EMSLAB Group, 1988. The EMSLAB electromagnetic sounding experiment, *EOS, Trans. Am. geophys. Un.,* **69,** 98–99.

Evans, R.L., Sinha, M.C., Constable, S.C. & Unsworth, M.J., 1994. On the electrical nature of the axial melt zone 13°N on the East Pacific Rise, *J. geophys. Res.,* **99,** 577–588.

Filloux, J.H., 1987. Instrumentation and experimental methods for oceanic studies, in *Geomagnetism,* Vol. 1, pp. 143–248, ed. Jacobs, J.A., Academic Press, New York.

Heinson, G.S. & Lilley, F.E.M., 1993. An application of thin-sheet electromagnetic modelling to the Tasman Sea, *Phys. Earth planet. Inter.,* **81,** 231–251.

Heinson, G.S., White, A., Law, L.K., Hamano, Y., Utada, H., Yukutake, T., Segawa, J. & Toh, H., 1993. EMRIDGE: the electromagnetic investigation of the Juan de Fuca Ridge, *Mar. Geophys. Res.,* **15,** 77–100.

Mackie, R.L., Smith, J.T. & Madden, T.R., 1994. Three-dimensional electromagnetic modeling using finite difference equation: the magnetotelluric example, *Radio Sci.,* **29,** 923–935.

Madden, T.R. & Mackie, R.L., 1989. Three-dimensional magnetotelluric modeling and inversion, *Proc. IEEE,* **77,** 318–333.

McKirdy, D.McA., Weaver, J.T. & Dawson, T.W., 1985. Induction in a thin-sheet of variable conductance at the surface of a stratified earth—II. Three-dimensional theory, *Geophys. J. R. astr. Soc.,* **80,** 177–194.

Nolasco, R., Tarits, P., Filloux, J.H. & Chave, A.D., 1998. Magnetotelluric imaging of the Society Islands hotspot, *J. geophys. Res.,* **103,** 30 287–30 309.

Price, A.T., 1949. The induction of electric currents in non-uniform thin-sheets and shells, *Quart. J. Mech. App. Math.,* **2,** 283–310.

Wannamaker, P.E., Stodt, J.A. & Rijo, L., 1986. Two-dimensional topographic responses in magnetotellurics modeled using finite elements, *Geophysics,* **51,** 2131–2144.

Wannamaker, P.E., Stodt, J.A. & Rijo, L., 1987. A stable finite element solution for two-dimensional magnetotelluric modelling, *Geophys. J. R. astr. Soc.,* **88,** 277–296.

Wannamaker, P.E., Booker, J.R., Jones, A.G., Chave, A.D., Filloux, J.H., Waff, H.S. & Law, L.K., 1989. Resistivity cross section through the Juan de Fuca subduction system and its tectonic implications, *J. geophys. Res.,* **94,** 14 127–14 144.

Wessel, P. & Smith, W.H., 1998. New, improved version of the Generic Mapping Tools released, *EOS, Trans. Am. geophys. Un.,* **79,** 579.